Simulating the Effects of "M-current" Potassium Channels in Cochlear Implant Excitation of Auditory Nerve Fibers

Ian C. Bruce[1], Laura Green[1], Babak V-Ghaffari[2] and Mark A. Rutherford[2]

[1]Department of Electrical & Computer Engineering, McMaster University, Hamilton, ON, Canada

[2]Department of Otolaryngology, Washington University School of Medicine, St. Louis, MO, USA

Abstract

Having an accurate description of the patterns of action potentials (APs) generated in auditory nerve fibers (ANFs) by cochlear implant (CI) stimulation is a crucial component to relating stimulation strategies to perceptual outcomes. Biophysical computational models are a powerful tool for capturing what is known about the electrochemical dynamics and ion-channel gating mechanisms underlying neural excitability.

Previous computational models of an ANF node of Ranvier suggest that low-threshold potassium (KLT) and hyperpolarization-activated cyclic nucleotide-gated cation (HCN) channels affect an ANF's absolute and relative refractory periods and produce adaptation/accommodation to high-rate pulse trains (Boulet and Bruce, 2017; Negm and Bruce, 2014). In this study we explore the effects of another type of potassium channel that has recently been identified in mammalian auditory nerve fibers, "M-current" potassium channels formed by $K_v7.2$ and $K_v7.3$ ion channel proteins (Kim and Rutherford, 2016). Like the KLT and HCN channels, the M current is active at the resting membrane potential of ANFs and has slower opening/closing dynamics than the AP-generating sodium and potassium channels. Thus, the M current is expected to also have an influence over the refractory, facilitation, accommodation and adaptation behavior of ANFs.

We have incorporated an M-current model used in other cell types (Lawrence et al., 2006) into the previous ANF model of Boulet and Bruce (2017). As a first step of evaluating this new model, we have compared simulation results to the room-temperature ANF patch-clamp data of Rutherford et al. (2012). This new model incorporating the M current is able to better predict these patch-clamp data in general. Further refinement of free parameters in the model is ongoing. The next step we are taking is to expand this model to describe extracellular CI stimulation of ANFs at mammalian body temperature.

I. INTRODUCTION

- As illustrated in Fig. 1, ANFs have a diversity of voltage-gate ion channels that have specific locations and densities along the length of the fiber (Hossain et al., 2005; Kim and Rutherford, 2016; Yi et al., 2010).

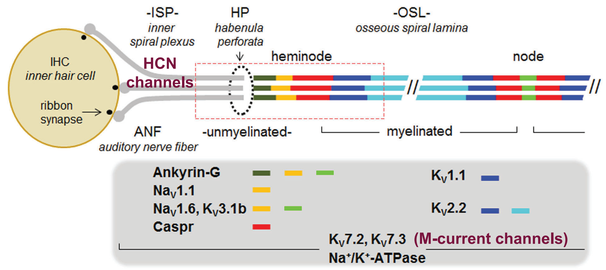

Figure 1: Locations of voltage-gated ion channels and anchoring proteins along the length of ANFs. Adapted from Kim and Rutherford (2016). **$K_v7.2$ & $K_v7.3$ → M-current**.

- Rutherford et al. (2012) performed patch-clamp recordings on the unmyelinated post-synaptic terminals of ANFs in excised rat cochleas. Example current-clamp recordings from p11 rats are shown in Fig. 2.

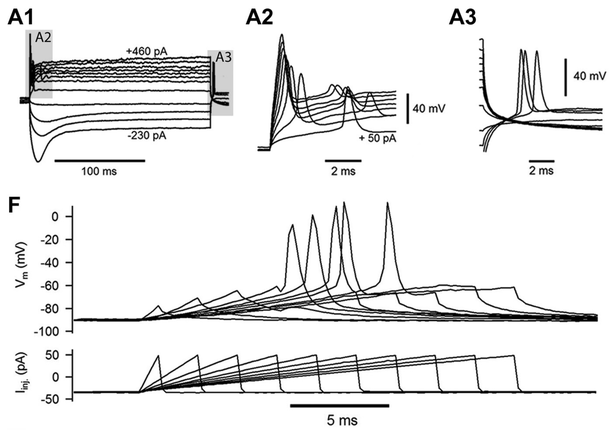

Figure 2: ANF patch-clamp recordings from Rutherford et al. (2012). A1: Responses to 200-ms current steps for a range of negative and positive current amplitudes. A2 & A3: Magnified plots of the onset and offset responses, respectively. F: Responses to ramp currents of varying durations in a different cell.

- Ramped electric stimuli may be of particular interest in CI stimulation because it has been argued that they might lead to improved spatial selectivity compared to the rectangular pulses that are presently used in clinical CIs (Ballestero et al., 2015).

II. MODEL STRUCTURE

- As shown in Fig. 3, the model used in this study is a stochastic version of the Hodgkin–Huxley (HH) parallel-conductance formulation for the action of voltage-gated ion channels on a patch of neural membrane. The previous ANF model of Boulet and Bruce (2017) incorporated HCN & KLT channels in addition to the standard HH model Na_v and K_v channels. In the proposed model, we include an M-current model used in other cell types (Lawrence et al., 2006).
- For consistency with the previous model, the $Na_v1.1$ and $K_v1.6$ channels and the $K_v2.2$ and $K_v3.1b$ channels from Fig. 1 are each lumped together into Na_v and K_v channels modified from the HH model. The KLT channel in the model describes the properties of the $K_v1.1$ and other low-threshold potassium channels in ANFs.

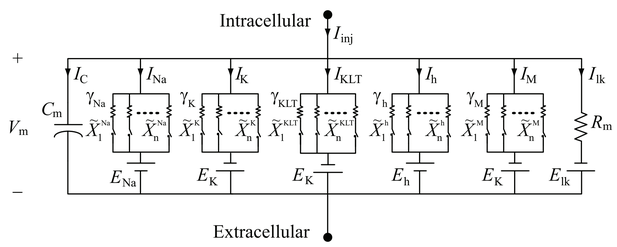

Figure 3: Electrical circuit model of the lumped membrane properties for patch-clamp recordings made at the ANF terminal onto the IHC.

- Table 1 provides preliminary sets of model parameters that have been found to generally describe the response properties of two cells from Rutherford et al. (2012), 'Cell 2010-09-21' and 'Cell 2010-10-05', both from p11 rats.
- Ion channel conductances and gating particle kinetics (see Fig. 4) were modified from Boulet and Bruce (2017) and Lawrence et al. (2006) because the recordings of Rutherford et al. (2012) were performed at room temperature rather than mammalian body temperature.
- The membrane capacitance and resting membrane input resistance for each cell were based on estimates from the respective patch-clamp experiments.
- The leakage current resistance and reversal potential were then adjusted for each model variant to obtain the required resting input resistance for that cell and to maintain the desired resting membrane potential.

Table 1: Membrane model parameters.

Parameter	Symbol	Cell 2010-09-21	Cell 2010-10-05
Cell temperature	T	22 °C	22 °C
Membrane capacitance	C_m	6 pF	4.5 pF
Input resistance	R_{in}	500 MΩ	750 MΩ
Leakage resistance	R_m	Model specific	Model specific
Na reversal potential	E_{Na}	120 mV	120 mV
K reversal potential	E_K	–88 mV	–88 mV
HCN reversal potential	E_h	–41 mV	–41 mV
Leakage potential	E_{lk}	Model specific	Model specific
Resting membrane pot.	V_{rest}	–78 mV	–78 mV
Na_v conductance	γ_{Na}	7.47 pS	7.47 pS
K_v conductance	γ_K	16.5 pS	16.5 pS
KLT conductance	γ_{KLT}	4.29 pS	4.29 pS
HCN conductance	γ_h	4.29 pS	4.29 pS
M conductance	γ_M	4.95 pS	4.95 pS
Max# Na_v channels	N_{Na}^{max}	10 000	10 000
Max# K_v channels	N_K^{max}	166	166
Max# KLT channels	N_{KLT}^{max}	166	166
Max# HCN(q) channels	$N_{h,q}^{max}$	447	447
Max# HCN(s) channels	$N_{h,s}^{max}$	553	553
Max# M channels	N_M^{max}	100–1000	100–1000
HCN(q) half-activation pot.	$V_{1/2,q}$	–91.72 mV	–91.72 mV
HCN(s) half-activation pot.	$V_{1/2,s}$	–90.33 mV	–90.33 mV
M half-activation pot.	$V_{1/2,M}$	–27 mV	–27 mV

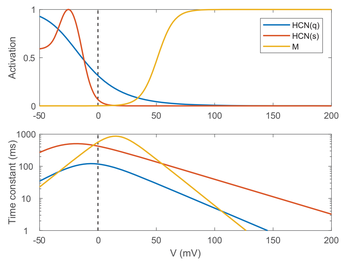

Figure 4: HCN and M-current gating particle activation functions (top panel) and time constants (bottom panel) as a function of the relative transmembrane potential ($V = V_m - V_{rest}$).

III. RESULTS

- Figure 5 shows example ANF responses of Cells 2010-09-21 & 2010-10-05 to hyperpolarizing and depolarizing current steps along with predictions for different model variants.

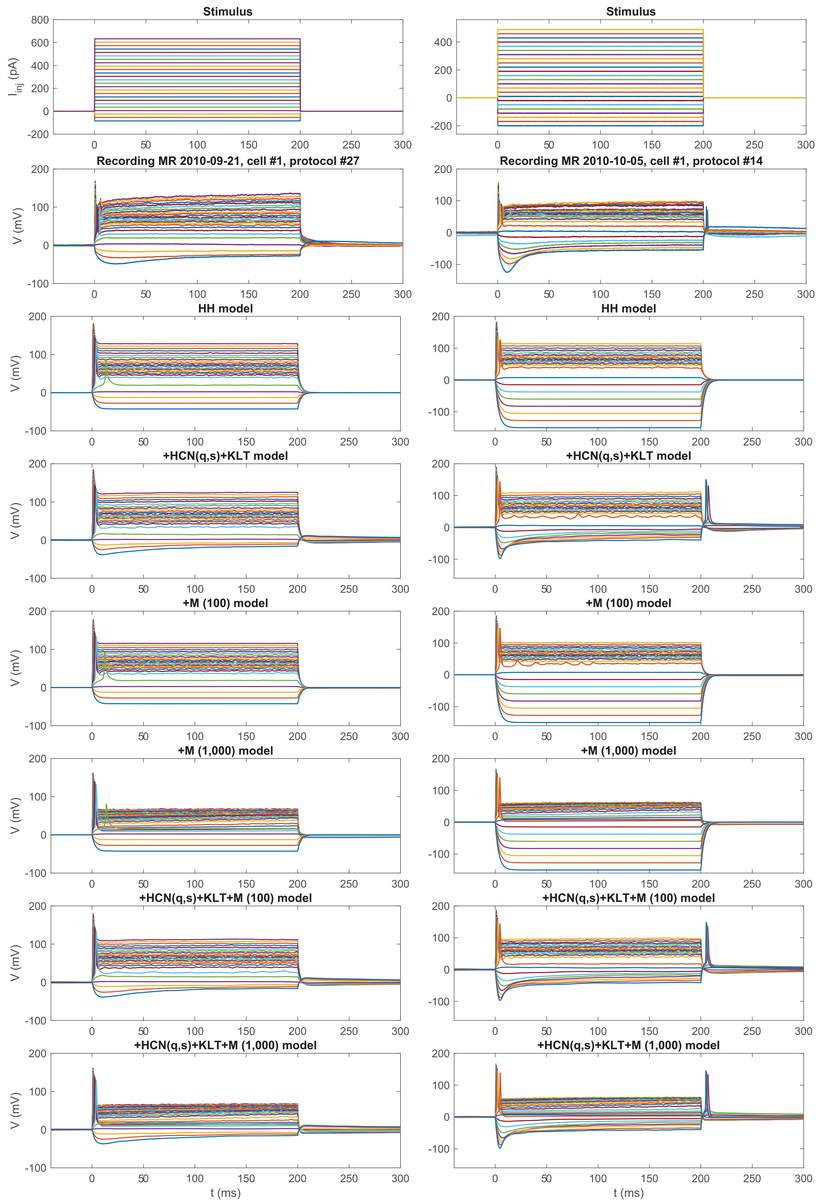

Figure 5: Data and model predictions for Cell 2010-09-21 (left column) and Cell 2010-10-05 (right column) in response to 200-ms current steps. The HH model incorporates just the Na_v and K_v channels. Other model variants include different combinations of additional channels, as indicated in the panel title. The number in parentheses indicates the number of M-current channels.

- Figure 6 shows example ANF responses of Cell 2010-09-21 to short and long current ramp durations along with predictions for different model variants.

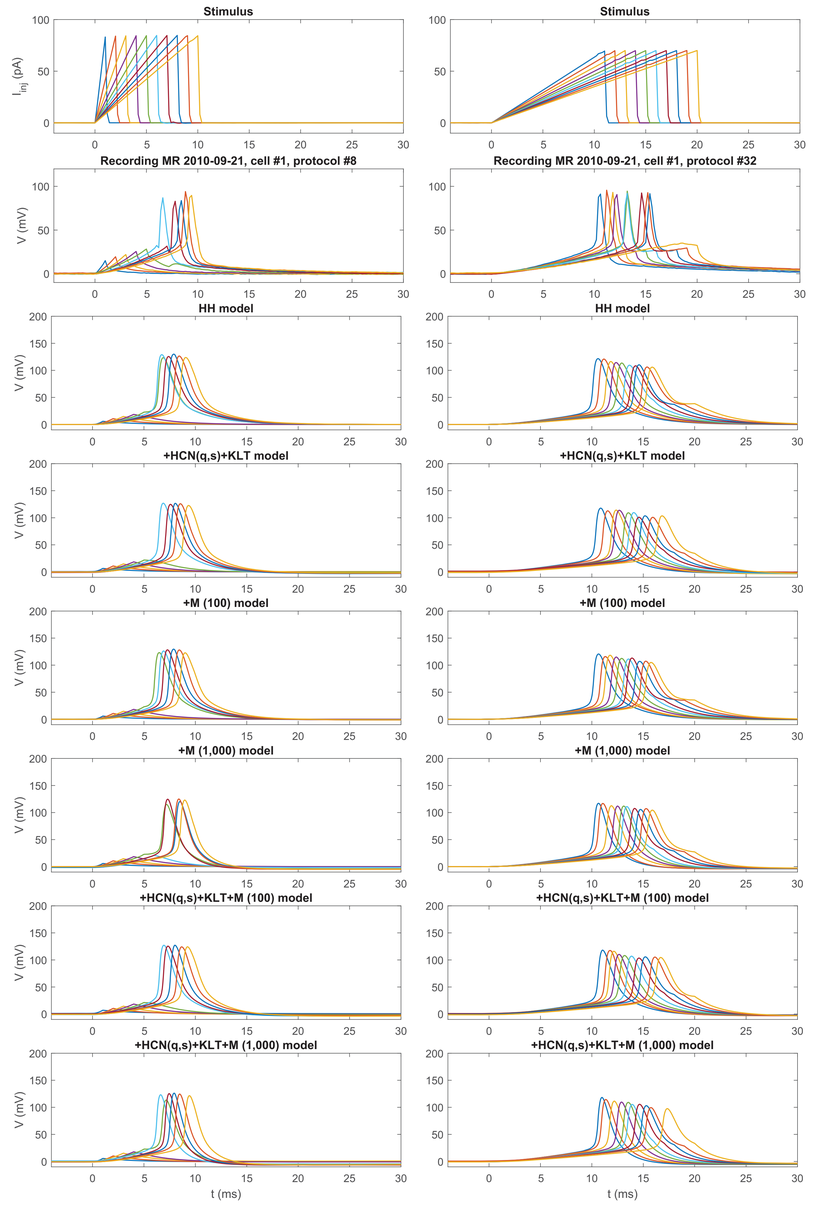

Figure 6: Data and model predictions for a cell's response to short (left column) and long (right column) ramped currents.

IV. DISCUSSION AND CONCLUSIONS

- Overall, the model with KLT & HCN channels and 100 M-current channels appears to best predict the example data. For step stimuli, the +HCN(q,s)+KLT+M (100) model best describes:
  1. the current amplitude at which spiking begins,
  2. the sag in hyperpolarization,
  3. the magnitude of the sustained depolarization following an onset spike, and
  4. the occurrence of hyperpolarization-rebound spikes for Cell 2010-10-05.

  For ramp stimuli, the +HCN(q,s)+KLT+M (100) model best describes:
  1. the ramp duration at which spiking begins (6 ms), and
  2. the jitter in spike latencies.
- None of the model variants predict the failure to spike in response to the 20-ms long ramp stimulus. However, the +HCN(q,s)+KLT+M (1,000) model does have a much longer spike latency in response to the 20-ms long ramp compared to the other model variants, indicating that it may be close to spike failure. Further exploration of M-current model parameters may be warranted.
- Alternatively, improved Na_v and K_v models based on the actual channels identified in mammalian ANFs (see Fig. 1) may be required to explain spike failure for long ramps and the small second spikes that are sometimes observed in onset responses to step stimuli (see Fig. 2A2).

REFERENCES

Ballestero, J., Recugnat, M., Laudanski, J., Smith, K. E., Jagger, D. J., Gnansia, D., and McAlpine, D. (2015). Reducing current spread by use of a novel pulse shape for electrical stimulation of the auditory nerve. *Trends Hear.*, 19:1–12.

Boulet, J. and Bruce, I. C. (2017). Predictions of the contribution of HCN half-maximal activation potential heterogeneity to variability in intrinsic adaptation of spiral ganglion neurons. *J. Assoc. Res. Otolaryngol.*, 18(2):301–322.

Hossain, W. A., Antic, S. D., Yang, Y., Rasband, M. N., and Morest, D. K. (2005). Where is the spike generator of the cochlear nerve? Voltage-gated sodium channels in the mouse cochlea. *J. Neurosci.*, 25(29):6857–6868.

Kim, K. X. and Rutherford, M. A. (2016). Maturation of Na_v and K_v channel topographies in the auditory nerve spike initiator before and after developmental onset of hearing function. *J. Neurosci.*, 36:2111–2118.

Lawrence, J. J., Saraga, F., Churchill, J. F., Statland, J. M., Travis, K. E., Skinner, F. K., and McBain, C. J. (2006). Somatodendritic Kv7/KCNQ/M channels control interspike interval in hippocampal interneurons. *J. Neurosci.*, 26:12325–12338.

Negm, M. H. and Bruce, I. C. (2014). The effects of HCN and KLT ion channels on adaptation and refractoriness in a stochastic auditory nerve model. *IEEE Trans. Biomed. Eng.*, 61(11):2749–2759.

Rutherford, M. A., Chapochnikov, N. M., and Moser, T. (2012). Spike encoding of neurotransmitter release timing by spiral ganglion neurons of the cochlea. *J. Neurosci.*, 32:4773–4789.

Yi, E., Roux, I., and Glowatzki, E. (2010). Dendritic HCN channels shape excitatory postsynaptic potentials at the inner hair cell afferent synapse in the mammalian cochlea. *J. Neurophysiol.*, 103(5):2532–2543.

ibruce@ieee.org

Supported by NSERC Discovery Grant #RGPIN-2018-05778 (ICB), NIH/NIDCD R01DC014712 (MAR), and a Hearing Health Foundation Fellowship (BV-G).